Photoluminescence of Bi^{3+} in $Y_3Ga_5O_{12}$ single-crystal host

2005 J. Phys.: Condens. Matter 17 3367

(http://iopscience.iop.org/0953-8984/17/21/029)

INSTITUTE OF PHYSICS PUBLISHING JOURNAL OF PHYSICS: CONDENSED MATTER

J. Phys.: Condens. Matter **17** (2005) 3367–3375 doi:10.1088/0953-8984/17/21/029

Photoluminescence of Bi^{3+} in $Y_3Ga_5O_{12}$ single-crystal host

M Nikl[1], A Novoselov[2], E Mihoková[1], K Polák[1], M Dusek[1], B McClune[3], A Yoshikawa[2] and T Fukuda[2]

[1] Institute of Physics AS CR, Cukrovarnicka 10, 162 53 Prague, Czech Republic
[2] Institute of Multidisciplinary Research for Advanced Materials, Tohoku University, 2-1-1 Katahira, Aoba-ku, Sendai 980-8577, Japan
[3] Clarkson University, Potsdam, NY 13 699-5820, USA

Received 28 February 2005, in final form 5 April 2005
Published 13 May 2005
Online at stacks.iop.org/JPhysCM/17/3367

Abstract

Photoluminescence spectra and decay kinetics within 10–350 K were measured in the Bi-doped $Y_3Ga_5O_{12}$ single crystal prepared by the micro-pulling-down technique. Temperature dependences of the decay times and the integrated emission intensities obtained from the experiment were simulated using a phenomenological two-excited-state-level model. The model provided quantitative parameters of the involved excited state levels of the Bi^{3+} luminescence centre in this host. The results are discussed in the light of already published data obtained for other Bi-doped compounds. The influence of the defects and structural irregularities of the host on the Bi^{3+} emission characteristics is discussed as well.

(Some figures in this article are in colour only in the electronic version)

1. Introduction

The Bi^{3+} ion belongs to the group of so called heavy ns^2 ions (Tl^+, Pb^{2+} and Bi^{3+}), the luminescence of which has been studied in a considerable number of hosts. Especially in the case of Tl^+, easily doped in alkali halides, there is an extensive number of experimental as well as theoretical studies published; for reviews, see [1, 2]. The Bi^{3+} centre also started to be studied more systematically in the 1970s and 1980s. Mainly oxide-based materials were adopted as the host due to better availability of trivalent sites, which were suitable for Bi^{3+} doping; see the reviews [3, 4]. With respect to Tl^+ and Pb^{2+}, more reports, dealing with the luminescence of Bi^{3+} centres, appear in the literature in recent years. New materials are sought for lighting applications, where high conversion and luminescence efficiency of employed phosphors is required up to temperature over 100–200 °C [5, 6]. Due to the variable valence of the Bi ion, Bi^{2+} luminescence was also reported and the coexistence of both the Bi^{2+} and Bi^{3+} centres can be found, for example, in $BaSO_4$:Bi [7]. Finally, in some cases the 'anomalous' emission

of Bi^{3+} was noticed and explained as due to an exciton bound around the Bi^{3+} ion, e.g. in an $La_2Zr_2O_7$ host [8], following the explanations adopted for similar situations of the Tl^+ centre in CsI:Tl [9] or Pb^{2+}-doped $CdCl_2$ [10].

The $Y_3Ga_5O_{12}$ (YGG) single crystal has been doped by several different rare earths and other ions in the search for solid state laser materials (Nd^{3+} doped in [11]), for up-conversion materials (Cr^{3+} and Yb^{3+} doped in [12]) or for scintillators (Yb^{3+} doped in [13]). However, to our knowledge, no study of luminescence of the Bi^{3+} centre in the YGG single crystal grown by classical Czochralski or Bridgman techniques is available in the literature. There is a considerable vapour pressure of Bi_2O_3 in the high temperature melt, resulting in its evaporation and therefore impossibility to achieve a reasonable concentration of Bi ion in the growing crystal. Recently, such a YGG:Bi single crystal was grown using a novel 'micro-pulling-down' technique [14]. Its scintillator efficiency at room temperature appears competitive to the classical $Bi_4Ge_3O_{12}$ (BGO) scintillator [15].

It is the aim of this paper to report luminescence characteristics of the Bi^{3+} centre in YGG in a wide temperature region, 10–350 K. Quantitative parameters of the excited state dynamics of Bi^{3+} are calculated within the framework of the two-excited-state-level phenomenological model. The model provides a satisfactory fit of the experimentally obtained temperature dependence of both the decay time and emission intensity.

2. Experimental details

Rod-shaped single crystals of the undoped and Bi-doped $Y_3Ga_5O_{12}$ were grown by the micro-pulling-down method. The dimension of the rods was typically ∅ 4 mm × 20 mm. They were transparent, without cracks and visible inclusions; for further details see [15]. A single phase with garnet structure and no impurity phases was observed. Chemical analysis showed 0.047 mol% of Bi in the YGG:Bi sample selected for this study. Plates of about 4 mm × 8 mm × 1 mm were cut and polished for the absorption and luminescence measurements.

Absorption spectra were measured with a Shimadzu UV-3101PC UV–VIS–NIR spectrophotometer at room temperature (RT) and at 80 K. Measurements of photoluminescence were performed within 10–350 K using liquid helium flow (10–300 K) and liquid nitrogen bath (80–350 K) optical cryostats from Oxford Instruments. A spectrofluorometer 199S (Edinburgh Instruments) was used for the luminescence experiment. It was equipped with a steady-state hydrogen flash-lamp, pulsed xenon microsecond flash-lamp and nanosecond hydrogen-filled flash-lamp as excitation sources. A single-grating emission monochromator and a Peltier-cooled TBX-04 detection module (IBH Scotland) working in photon counting mode were used in the detection part. All the spectra were corrected for experimental distortions. Luminescence decay kinetics within the ns–ms timescale was measured with the same set-up using

(i) the microsecond xenon flash-lamp and detection by multichannel analyser in the scaling mode for slow decay processes and
(ii) the nanosecond hydrogen-filled coaxial flash-lamp and time-correlated single-photon counting method for fast decay processes.

Deconvolution procedures (Spectra-Solve software from LASTEK) were used to extract true decay times in the situation when the decay curves were distorted due to the finite width of the instrumental response.

3. Experimental results

When the YGG host is doped with Bi^{3+}, the absorption band at 285 nm, displayed in figure 1, appears. This band has been already reported in the literature [16] and ascribed to the lowest

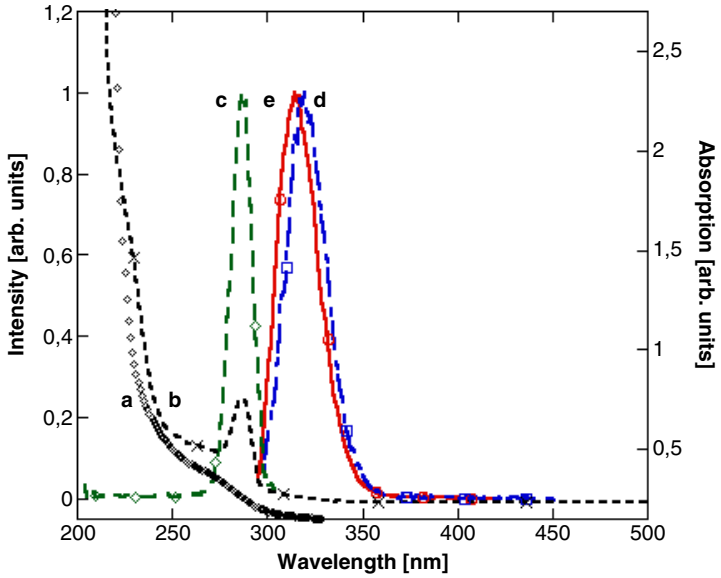

Figure 1. Absorption (a), (b), excitation (c) and emission (d), (e) spectra of YGG:Bi10%: (a) undoped YGG, RT; (b) Bi doped, 80 K; (c) $\lambda_{em} = 320$ nm, 80 K; (d) $\lambda_{ex} = 285$ nm, 80 K; (e) $\lambda_{ex} = 285$ nm, 142 K.

energy $6s^2 \rightarrow 6s6p$ transition of Bi^{3+}. Excitation within this absorption band produces a luminescence band at 315–320 nm (see figure 1), only recently reported and ascribed to the radiative transition of the excited Bi^{3+} centre in YGG host [15]. Below 100 K this emission peaks at 320 nm, while between 130 and 140 K it is shifted to higher energies by about 0.08 eV; see figure 1.

Below 70 K the luminescence decay of the 320 nm band follows a single-exponential course and shows the decay time of about 1.1–1.2 ms; see figure 2(a). The very first point (50 μs-per-point time resolution) of the decay curve shows noticeably higher value. Using time-correlated single-photon counting and the nanosecond flash-lamp excitation, the decay measurement within a submicrosecond timescale has shown another, fast, component (FC). It has rather low intensity and two decay times of about 2 and 25 ns can be resolved in the decay curve at 9 K; see figure 2(b). Under the same excitation, time-resolved (0–500 ns time gate) and steady-state emission spectra were recorded at 8 K to obtain the intensity ratio of the fast and slow decay components—the inset of figure 2(b). The emission intensity of FC is about 2–3% of the total lightsum and the emission maximum is clearly high-energy shifted with respect to the steady-state spectrum by about 0.1 eV. The temperature dependence of the slow component (SC) decay time is shown in figure 3(a). Above 70 K the decay accelerates, reaching about 300–350 ns at the room temperature. It is interesting to note that in the low energy part of the emission band around 340 nm the SC decay time values are systematically lower by about 10–15% and in the temperature region of acceleration above 100 K the decay starts to slightly deviate from a single-exponential course. To get the temperature dependence in figure 3(a) the decay times were extracted from the tails of the curves measured at 310 nm.

The temperature dependence of the emission intensity was constructed from the integrals of the emission spectra measured under 285 nm excitation (examples in figure 1) and is given in figure 3(b). A pronounced intensity decrease appeared above 200 K, i.e. at much higher temperatures with respect to the knee at the dependence of the decay times in figure 3(a).

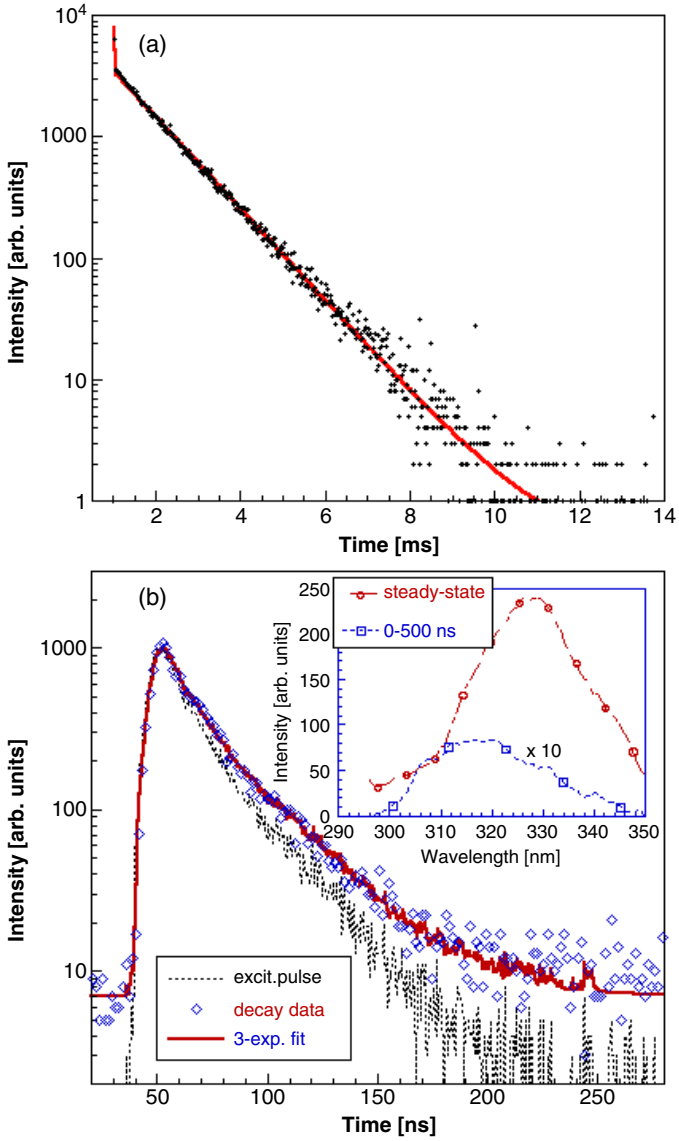

Figure 2. (a) Photoluminescence decay of the slow component, YGG:Bi10%, $\lambda_{exc} = 285$ nm, $\lambda_{em} = 320$ nm, $T = 12$ K. The solid line is a two-exponential fit by the function $I(t) = 4400 \times \exp[-t/0.001\ \text{ms}] + 3397 \times \exp[-t/1.15\ \text{ms}] + 0.43$. (b) Photoluminescence decay of the fast component, YGG:Bi10%, $\lambda_{exc} = 285$ nm, $\lambda_{em} = 310$ nm, $T = 9$ K. The solid line is the convolution of the instrumental response to the excitation pulse and the function $I(t) = 32\,870 \times \exp[-t/0.1\ \text{ns}] + 3390\exp[-t/2.0\ \text{ns}] + 160 \times \exp[-t/25\ \text{ns}] + 7$. The first component of the 0.1 ns decay time stands for the scattered excitation light and has no physical meaning. In the inset the steady-state and time-resolved (0–500 ns gate) emission spectra are given under the excitation $\lambda_{exc} = 285$ nm using the nanosecond pulse flash-lamp.

4. Phenomenological model

The excited state dynamics of the Bi^{3+} centre is given by two optically active electrons in the 6s shell, which undergo the (lowest of) $6s^2 \leftrightarrow 6s6p$ transition(s) under the excitation within

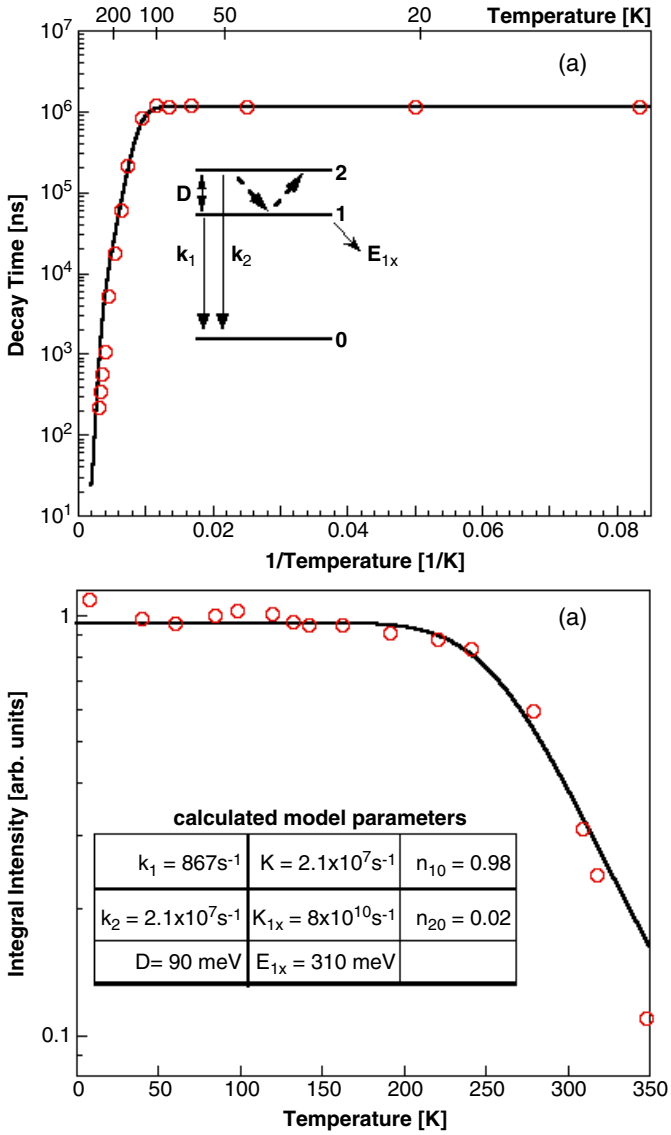

Figure 3. (a) Temperature dependence of the decay times ($\lambda_{exc} = 285$ nm, $\lambda_{em} = 310$ nm); (b) temperature dependence of the integrated emission intensities ($\lambda_{exc} = 285$ nm). The inset of (a) displays a sketch of the two-excited-state-level phenomenological model. The levels 0, 1 and 2 correspond in the D_2 symmetry to the ground state A_1 and excited states A_2 and E, respectively. (The same scheme applies as well for the O_h symmetry where the levels 0, 1 and 2 would correspond to $^1A_{1g}$, $^3A_{1u}$ and $^3T_{1u}$.) The model is employed to describe the excited state dynamics of the luminescence centre. Solid lines are calculated from the model; symbols represent experimental data. Calculated parameters of the model are reported in (b); see also the text for more details.

the 285 nm absorption band. The excited 6s6p configuration has a spin allowed ^1P and spin forbidden ^3P levels. In a cubic crystal field (referring to the case of ns^2 ions in alkali halides) these transform in the $^3A_{1u}$, $^3T_{1u}$, $^3T_{2u}$ and $^1T_{1u}$. The lowest excited state of the emission centre consists of the triply degenerate $^3T_{1u}$ level and the close underlying $^3A_{1u}$ level. While the transition from the $^3A_{1u}$ level to the $^1A_{1g}$ ground state is strongly forbidden, transition from

$^3T_{1u}$ is partially allowed due to spin–orbit mixing with the $^1T_{1u}$ level. Based on this excited state level arrangement the phenomenological models were applied to the isoelectronic Tl^+ centre in alkali halide hosts and quantitative parameter values were determined [17, 18]. In the present case the symmetry of the Bi^{3+} centre is D_2 (see below) and the lowest excited state of the centre consists of the E level and underlying level A_2. A similar model as for the Tl^+ centre can be applied. The model is sketched in figure 3(a). The time development of the populations N_1 and N_2 of the excited levels 1 (A_2) and 2 (E), respectively, can be described by the following equations:

$$\begin{aligned} dN_1/dt &= -k_1N_1 - k_{12}N_1 + k_{21}N_2 - k_{1x}N_1 \\ dN_2/dt &= -k_2N_2 - k_{21}N_2 + k_{12}N_1, \end{aligned} \tag{1}$$

where k_1, k_2, k_{12}, k_{21} and k_{1x} are radiative transition rates from levels 1 and 2 and non-radiative rates of phonon assisted transitions between the radiative level 2 and metastable level 1 and the quenching channel from the level 1, respectively. Non-radiative transitions between levels 1 and 2 can be written as

$$k_{21} = K(n+1), \qquad k_{12} = Kn, \qquad n = 1/[\exp(D/k_BT) - 1]. \tag{2}$$

Here K, n and D are the zero-temperature transition rate between the levels 1 and 2, the Bose–Einstein factor [19] and the energy spacing between the levels, respectively. The non-radiative quenching channel is considered in the usual barrier form:

$$k_{1x} = K_{1x}\exp(-E_{1x}/k_BT) \tag{3}$$

with K_{1x} being a frequency factor and E_{1x} the height of the barrier. This model was used to fit the experimental data of both the temperature dependence of decay times and integral intensity in figures 3(a) and (b), respectively. The values of some parameters, namely k_1, $k_2 + K$ and the ratio of the initial populations of levels 1 (n_{10}) and 2 (n_{20}), were determined directly from the experiment as reciprocal asymptotic values of measured slow and fast decay times (figures 2(a) and (b)) and the relative intensity of the time-resolved emission spectrum (inset of figure 2(b)), respectively. The remaining parameters of the model were determined from the best fit of the data and are summarized in figure 3(b).

5. Discussion

Obtained parameters in figure 3(b) allow a quantitative comparison with luminescence characteristics of other Bi-doped materials. It was found by Blasse and van der Steen [20] that the lower Stokes shift results in larger energy separation between levels 1 and 2 (parameter D in the model). For instance, in CaO:Bi^{3+} the Stokes shift was found to be 0.4 eV and $D = 0.15$ eV, while for La_2O_3:Bi the values 1.35 and 0.046 eV, respectively, were obtained. In another study [21], the Bi-doped $ScBO_3$ and $LaBO_3$ luminescence characteristic evaluation provided the values of the Stokes shift 0.22 and 1.16 eV and related energy separations $D = 0.12$ and 0.055 eV, respectively. It was concluded that the smaller coordination number (an octahedral site) and smaller size of the trivalent ion which Bi^{3+} is substituting for result in a smaller Stokes shift. In the YGG host the point symmetry of the dodecahedral Y^{3+} (Bi^{3+}) site is D_2 [22] and it is surrounded by eight oxygen ligands in a distorted cube arrangement—figure 4. Despite the higher coordination number, a relatively small Stokes shift of 0.37 eV is obtained, which is evaluated from maxima of the excitation and emission spectra at 80 and 140 K, respectively, in figure 1. An energy separation of levels 1 and 2, $D = 90$ meV is obtained (see calculated parameters in figure 3(b)). The relation between the values of the Stokes shift and parameter D is compatible with results and conclusions of [20, 21]. Apparently, about 10–15% smaller Y^{3+} size with respect to the Bi^{3+} ionic radius (Bi^{3+}(VIII) = 1.17 Å, Y^{3+}(VIII) = 1.019 Å)

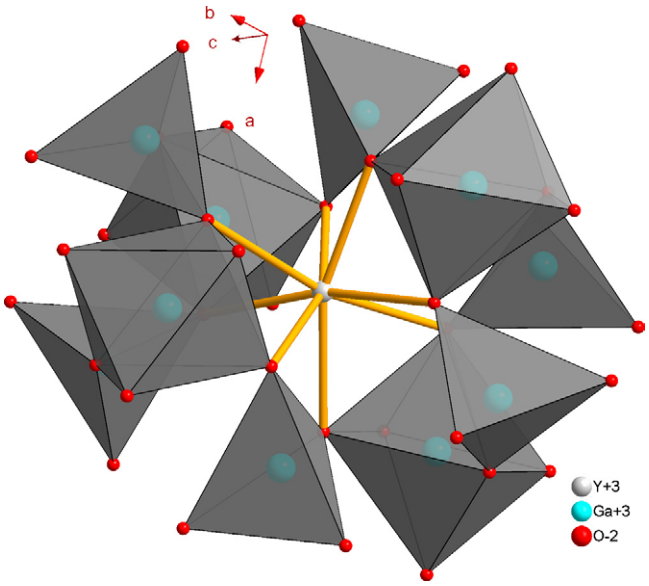

Figure 4. A sketch of the $Y_3Ga_5O_{12}$ structure.

prevents Bi^{3+} from an off-centre positioning [21], which would result in an enhanced Stokes shift and more serious emission quenching.

In earlier studies of Bi^{3+} luminescence no attention was paid to the fast emission from the upper level (E in D_2 symmetry, level 2 in our model). At low temperatures its intensity depends on the initial population of this level and the ratio of k_2 and K rate constants. In YGG:Bi the longer decay time obtained in the FC decay at 8 K is about 24 ns (see also the discussion below), which is fully comparable with the values found in the case of the isoelectronic Tl^+ or Pb^{2+} centres in alkali halides studied earlier by some of us [17, 18, 24, 25]. However, the fast emission intensity in YGG:Bi is extremely weak and performed calculations point to very small initial population of the (relaxed) upper level 2 (E) rather than to very small k_2/K ratio. Such a result is seemingly illogical, if one takes into account that a very dominant part in the absorption (excitation) transition within the 285 nm band is related to the transition $A_1 \rightarrow E$ ($0 \rightarrow 2$ in the model) at the Bi^{3+} centre. A very small initial population of level 2 (E) after the initial relaxation is also confirmed from the temperature dependence of the emission spectra between 80 and 140 K in figure 1: the high energy shift of the spectrum by about 80 meV is very close to the value of parameter $D = 90$ meV. At these temperatures, level 2 starts to be populated by thermal excitation of electrons from the underlying level 1 (A_2) and an increasing part of the emitted light comes from the transition $E \rightarrow A_1$ ($2 \rightarrow 0$). A similar high energy shift of the emission spectrum was also noticed in $ScBO_3$:Bi [20]. Poor initial population of level 2 (E) can be tentatively explained as due to a non-elementary character of the relaxation processes before the relaxed excited state is reached, which bring the major part of the excited electrons on the adiabatic potential energy surface of the underlying 1 (A_2) level. It is worth noticing that the complexity of these processes was stressed in a recent theoretical study of lattice relaxation around ns^2 luminescence centres in alkali halides [26], where among others the influence of covalency effects was also considered.

The observed two-component character of the FC decay deserves another comment. Due to the lowering of site symmetry by an adjacent compensating cationic vacancy in the case of Pb^{2+}-doped alkali halides, the splitting of the upper radiative level (level 2 in the sketch in

figure 3(a)) occurs and two components are resolved in the FC decay. Their decay times differ by about a factor of two [24]. In the present case the FC decay curve is approximated by two components of about 2 and 25 ns decay time. In the model calculations above the splitting of level 2 was not considered because of limited information available from experimental data. The origin of the 2 ns component is in question and could be tentatively explained in two ways.

(i) This component is related to the fast emission coming from Bi^{3+} centres located at the octahedral Ga site (see figure 4), considering that a concentration of the antisite Y_{Ga} centres in the YGG structure can reach a few per cent [27]. Shorter Bi–O distances at the octahedral site will result in an enhanced covalency of the chemical bond. Consequently, the singlet–triplet mixing will be increased and hence the FC lifetime will become shorter.
(ii) Lower static symmetry of the Y^{3+} site will result in larger splitting of the radiative excited state level (no 2) of the Bi^{3+} centre and thus a shorter radiative lifetime of the upper sublevel can be expected with respect to the situation observed in the case of Pb^{2+}-doped alkali halides mentioned above.

The thermal quenching of the Bi^{3+} luminescence can be evaluated in figure 3(b). The emission intensity at 280–285 K decreases to 50% of its low temperature value. Apparently, YGG:Bi cannot be considered for any high temperature applications, for example of YPO_4:Bi [6], where a 50% intensity reduction of the Bi^{3+} emission band occurs above 620 K. However, as far as the scintillator application is considered [15], the quantum efficiency of the Bi^{3+} centre in YGG at RT is noticeably higher (about 0.4, see figure 3(b)) with respect to that of BGO (about 0.13, see [24]), while its RT photoluminescence decay time is comparable with that of BGO.

The mentioned shorter decay time at the low energy side of the emission band and increasing non-exponentiality of the decay in the intermediate temperature region can be due to the point defects and structural irregularities in the YGG single-crystal host and/or Bi ion pair creation. The ns^2 ions are very sensitive to the irregularities in their surroundings because of the nature of their optical transitions ($ns^2 \rightarrow nsnp$) [1–4], so that the presence of any defects nearby can influence the position of both the ground- and excited-state levels. Consequently, the energy separation of excited-state levels can be affected and therefore the luminescence dynamics can be distorted especially in the region of the knee of the dependence in figure 3(a). Furthermore, Bi ion pairing in the YGG host [28] cannot be excluded, considering that the concentration of Bi ions in the crystal studied was about 500 ppm.

6. Conclusions

Doping the Bi^{3+} ion in the $Y_3Ga_5O_{12}$ lattice induces the additional absorption peak at 285 nm. Excitation within this absorption band provides the luminescence band centred around 315–320 nm in which two decay components were resolved. Related absorption and luminescence transitions are ascribed to electronic transitions between $6s^2 \leftrightarrow 6s6p$ configurations of Bi^{3+}. Temperature dependences of integrated luminescence intensity and decay times were successfully described in the framework of a two-excited-state-level phenomenological model. The value of the Stokes shift, 0.37 eV, and that of energy separation between the two excited state levels, $D = 90$ meV, are coherent with previously stated correlations between these two parameters in other Bi-doped compounds. Rather weak intensity observed for the fast nanosecond decay component is explained as a consequence of very low initial population of the upper excited state level arising due to the complex relaxation process before the relaxed excited state is formed. Decay kinetics distortion at the low energy side of the 320 nm emission band is ascribed to the influence of the nearby lying defects and/or Bi pairing in the YGG host.

Acknowledgments

This work was partially supported by the Industrial Technology Research Grant Programme 03A26014a from the New Energy and Industrial Technology Development Organization (NEDO) of Japan. Partial support of the Czech MSMT, KONTAKT, 1P2004ME716 and Institutional Research Plan No AV0Z10100521 projects is also gratefully acknowledged.

References

[1] Ranfagni A, Mugnai D, Bacci M, Viliani G and Fontana P 1983 *Adv. Phys.* **32** 823
[2] Jacobs P W M 1991 *J. Phys. Chem. Solids* **52** 35
[3] Boulon G 1987 *Spectroscopy of Solid-State Laser-type Materials* vol 30, ed B Di Bartolo (New York: Plenum) pp 223–66
[4] Blasse G 1988 *Prog. Solid State Chem.* **18** 79
[5] Guo P, Zhao F, Li G, Liao F, Tian S and Jing X 2003 *J. Lumin.* **105** 61
[6] Justel T, Huppertz P, Mayr W and Wiechert D U 2004 *J. Lumin.* **106** 225
[7] Gaft M, Reisfeld R, Panczer G, Boulon G, Saraidarov T and Erlish S 2001 *Opt. Mater.* **16** 279
[8] Sristava A M and Beers W W 1999 *J. Lumin.* **81** 293
[9] Nagirnyi V, Zazubovich S, Zepelin V, Nikl M and Pazzi G P 1994 *Chem. Phys. Lett.* **227** 533
[10] Moine B, Pedrini C and Ghiordanescu V 1994 *J. Phys.: Condens. Matter* **6** 4093
[11] Rukmini E and Jayasankar C K 1995 *Physica* B **212** 167
[12] Heer S, Wermuth M, Kramer K and Gudel H U 2002 *Phys. Rev.* B **65** 125112
[13] Kamenskikh I A, Guerassimova N, Dujardin C, Garnier N, Ledoux G, Pedrini C, Kirm M, Petrosyan A and Spassky D 2004 *Opt. Mater.* **24** 267
[14] Fukuda T 2004 Growth of micro and bulk crystals by modified micro-PD and their properties *Fiber Crystal Growth from the Melt* ed T Fukuda, P Rudolph and S Uda (Berlin: Springer) pp 255–81
[15] Novoselov A, Yoshikawa A, Nikl M, Solovieva N and Fukuda T 2005 *Cryst. Res. Technol.* **40** 419
[16] Lacklinson D E, Scott G B and Page J L 1974 *Solid State Commun.* **14** 861
[17] Hlinka J, Mihóková E and Nikl M 1991 *Phys. Status Solidi* b **166** 503
[18] Nikl M, Hlinka J, Mihóková E, Polák K, Fabeni P and Pazzi G P 1993 *Phil. Mag.* B **67** 627
[19] Marder M P 2000 *Condensed Matter Physics,* (New York: Wiley–Interscience) p 319
[20] Blasse G and van der Steen A C 1979 *Solid State Commun.* **31** 993
[21] Wolfert A, Oomen E W J L and Blasse G 1985 *J. Solid State Chem.* **59** 280
[22] Fischer P, Haelg W, Stoll E and Segmueller A 1966 *Acta Crystallogr.* **21** 765
[23] Melcher C L *et al* 1996 *Inorganic Scintillators and their Applications* ed P Dorenbos and C W E van Eijk Delft University Press, p 309
Melcher C L *et al* 1995 *Proc. SCINT 1995 (Delft, Netherlands, Aug. 1995)*
[24] Polák K, Nikl M and Mihóková E 1992 *J. Lumin.* **54** 189
[25] Hlinka J, Mihóková E, Nikl M, Polak K and Rosa J 1993 *Phys. Status Solidi* b **175** 523
[26] Andriessen J, Marsman M and van Eijk C W E 2001 *J. Phys.: Condens. Matter* **13** 10507
[27] Shirinyan G, Ovanesyan K L, Eganyan A, Petrosyan A G, Pedrini C, Dujardin C, Kamenskikh I and Guerassimova N 2005 *Nucl. Instrum. Methods Phys. Res.* A **537** 134
[28] Tsuboi T and Jacobs P W M 1991 *J. Phys. Chem. Solids* **52** 69